



Blocking Adipocyte YY1 Decouples Thermogenesis From Beneficial Metabolism by Promoting Spermidine Production

Chen Qiu,^{1,2,3} Yu Lu,¹ Suyang Wu,⁴ Wenli Guo,² Jiahao Ni,² Jiyuan Song,² Zichao Liu,⁵ Xiaoi Chang,² Kai Wang,^{6,7} Peng Sun,² Qian Zhang,⁵ Shufang Yang,^{1,8} and Kai Li^{1,2}

Diabetes 2025;74:295–307 | <https://doi.org/10.2337/db24-0501>

The accumulation of mitochondria in thermogenic adipose tissue (i.e., brown and beige fat) increases energy expenditure, which can aid in alleviating obesity and metabolic disorders. However, recent studies have shown that knocking out key proteins required to maintain mitochondrial function inhibits the energy expenditure in thermogenic fat, and yet the knockout (KO) mice are unexpectedly protected from developing obesity or metabolic disorders when fed a high-fat diet (HFD). In the current study, nonbiased sequencing-based screening revealed the importance of Yin Yang 1 (YY1) in the transcription of electron transport chain genes and the enhancement of mitochondrial function in thermogenic adipose tissue. Specifically, YY1 adipocyte-null (YAKO) mice showed lower energy expenditure and were intolerant to cold stress. Interestingly, YAKO mice showed alleviation of HFD-induced metabolic disorders, which can be attributed to a suppression of adipose tissue inflammation. Metabolomic analysis revealed that blocking YY1 directed glucose metabolism toward lactate, enhanced the uptake of glutamine, and promoted the production of anti-inflammatory spermidine. Conversely, blocking spermidine production in YAKO mice reversed their resistance to HFD-induced disorders. Thus, although blocking adipocyte YY1 impairs the thermogenesis, it promotes spermidine production, alleviates adipose tissue inflammation,

ARTICLE HIGHLIGHTS

- Chromatin open atlas profiling in white, beige, and brown adipocytes identified Yin Yang 1 (YY1) as a key transcription factor governing electron transport chain gene expression and mitochondrial function in thermogenic adipocytes.
- Knocking out adipocyte YY1 leads to impaired thermogenesis under cold stress while protecting the mice from diet-induced obesity and metabolic disorders.
- YY1-null adipocytes undergo metabolic reprogramming, with increased glutamine use and spermidine generation that combat adipose tissue inflammation and insulin resistance, resulting in an uncoupling of thermogenic capacity and metabolic benefits.

and therefore leads to an uncoupling of adipose tissue energy expenditure from HFD-induced metabolic disorders.

Brown and beige adipose tissues are considered thermogenic fats because they possess a unique ability to increase heat production by separating mitochondrial respiration from ATP synthesis. Consequently, a general consensus is

¹Department of Endocrinology, The Affiliated Taizhou People's Hospital of Nanjing Medical University, Taizhou School of Clinical Medicine, Nanjing Medical University, Taizhou, China

²Key Laboratory of Human Functional Genomics of Jiangsu Province, Nanjing Medical University, Nanjing, China

³Key Laboratory of the Model Animal Research, Animal Core Facility of Nanjing Medical University, Nanjing, China

⁴Department of Science and Technology, Jiangsu Cancer Hospital, The Affiliated Cancer Hospital of Nanjing Medical University, Jiangsu Institute of Cancer Research, Nanjing, China

⁵Department of Nutrition and Health, China Agricultural University, Beijing, China

⁶Endocrine and Metabolic Disease Medical Center, Drum Tower Hospital affiliated to Nanjing University Medical School, Nanjing, China

⁷Department of Medical Technology, Anhui Medical College, Hefei, Anhui, China

⁸School of Medicine, Southeast University, Nanjing, China

Corresponding authors: Qian Zhang, qianzhang@cau.edu.cn, Shufang Yang, yangsufang@njmu.edu.cn, and Kai Li, likai87@njmu.edu.cn

Received 17 June 2024 and accepted 25 November 2024

This article contains supplementary material online at <https://doi.org/10.2337/figshare.27909681>.

C.Q., Y.L., and S.W. contributed equally.

© 2024 by the American Diabetes Association. Readers may use this article as long as the work is properly cited, the use is educational and not for profit, and the work is not altered. More information is available at <https://www.diabetesjournals.org/journals/pages/license>.

that because thermogenic adipose tissues accumulate in mitochondria and enhance global energy expenditure (EE), they can protect the body from obesity and metabolic disorders caused by excessive energy intake (1–4). However, several recent investigations have revealed that under metabolic stresses, such as high-fat diet (HFD) feeding, the body may exhibit advantageous metabolism even in the presence of severe thermogenic adipose tissue dysfunction.

For example, knockout (KO) of *Lkb1* and *Tfam* expression, which promote mtDNA transcription in brown adipocytes (5), or elimination of *Mfn2* expression, which governs mitochondrial fusion (6), can block mitochondrial respiration and adipose thermogenesis in mice, and yet the KO animals show improved systemic metabolism when fed a HFD that would normally cause metabolic disorders. Similarly, knocking out thioredoxin-2 (*Trx2*), a key member of the mitochondrial thioredoxin system that neutralizes mitochondrial reactive oxygen species (mtROS), impairs adaptive thermogenesis in mice but improves their glucose and insulin sensitivity after HFD feeding (7). Collectively, these studies point to specific signals that inhibit the activation of thermogenic fat and yet somehow protect the mice from HFD-induced metabolic disorders. Whether this uncoupling of thermogenesis and metabolic benefits is just a coincidence or whether these processes have commonalities in their mechanisms of action remains unclear. However, all of the results seem to point to the involvement of mitochondria.

In the current study, we performed multiple sequencing-based assays and identified Yin Yang 1 (YY1) as an essential transcription factor that maintains the proper functioning of the mitochondrial electron transport chain (ETC) during adipose thermogenesis. Importantly, adipocyte YY1-null mice also demonstrated an uncoupling of thermogenic capacity and beneficial metabolism. We found that knocking out YY1 blocked the mitochondrial tricarboxylic acid (TCA) cycle and enhanced compensatory glutamine usage. Glutamine deamination generated spermidine (Spd), an anti-inflammatory metabolite, which reduced adipose tissue inflammation and insulin resistance caused by HFD feeding. Our results identified a specific mechanism centered on mitochondrial loss and metabolic reprogramming that is uncoupled from thermogenic capacity in adipose tissue and results in a beneficial metabolism phenotype.

RESEARCH DESIGN AND METHODS

Animal Models

YY1^{flox/flox} mice were a gift from Prof. Xiaoying Li (8). After crossing the flox mice with *adipoq*-cre mice (Jackson Laboratory), the male YY1 adipocyte KO mice (YY1^{flox/flox} * *adipoq*-cre, abbreviated YAKO) were compared with control male littermates (YY1^{flox/flox}, abbreviated Ycon). Male C57BL/6 J mice were purchased from the Animal Core Facility of Nanjing Medical University. Male *db/db* mice were purchased from the Model Animal Research Center of Nanjing University (Nanjing, China).

For adeno-associated virus (AAV)-induced gene knock-down, we purchased AAV viruses (YY1 shRNA-AAV8 and *Odc1* 4in1 shRNA-AAV8) from Vigene Bioscience (Shandong, China). The AAVs were injected into the inguinal white adipose tissue (iWAT) of male C57BL/6 J mice at three different sites (5 μ L per site, 1×10^{13} viral genomes/mL). A nonsense shRNA-AAV8 was used as a control. At 6 weeks after injection, the mice were imaged using the IVIS Spectrum in vivo imaging system (PerkinElmer, Waltham, MA).

For cold stress (CS)-induced thermogenesis, age-matched male littermates were subjected to cold stimulation (10°C for 6 h, then 4°C for 7 days) in a well-ventilated refrigerator. For the diet-induced obesity model, 4- to 5-week-old male YAKO mice and their Ycon counterparts were fed an HFD (60% kCal from fat; D12492, Research Diets) for 14 weeks. The mice were kept in a specific pathogen-free level facility at Nanjing Medical University and were provided with adequate food and water under normal light, temperature, and humidity conditions (12 h light/dark cycle, 60–70% humidity). All animal testing activities were conducted under the guidance of the Nanjing Medical University Institutional Animal Care and Use Committee (permit no. IACUC-1911030).

Statistical Analysis

The data are expressed as mean \pm SEM. Significant differences were assessed using a two-tailed Student *t* test or one-way ANOVA for multiple group comparisons. All data analysis was performed using GraphPad Prism 8 (GraphPad Software). A value of *P* < 0.05 was considered statistically significant.

Data and Resource Availability

The generated raw data sets, together with the analyzed bigwig and narrowpeak files generated during the current study, are available in the Gene Expression Omnibus repository as GSE234879 and GSE272637. An analysis was also performed using the existing public sequencing data GSE83764 from the Gene Expression Omnibus database. Other data sets generated and/or analyzed during the current study are available upon request. Other detailed method information is available in the Supplementary Material.

RESULTS

Adipocyte Open Chromatin Atlas

Thermogenic adipocytes respond to stimuli, such as cold exposure, by retaining mitochondria, making these cells ideal models for studying mitochondrial biogenesis. We conducted a high-throughput sequencing (seq) assay for transposase-accessible chromatin (ATAC-seq) in brown, beige, and white adipocytes derived from a stromal vascular fraction (SVF) to search for key proteins that govern the structure and function of mitochondria during thermogenesis (Fig. 1A). The sequencing data showed peak signals enriched at transcriptionally active DNA regions, such as exons, introns, and promoters (Supplementary Fig. 1A).

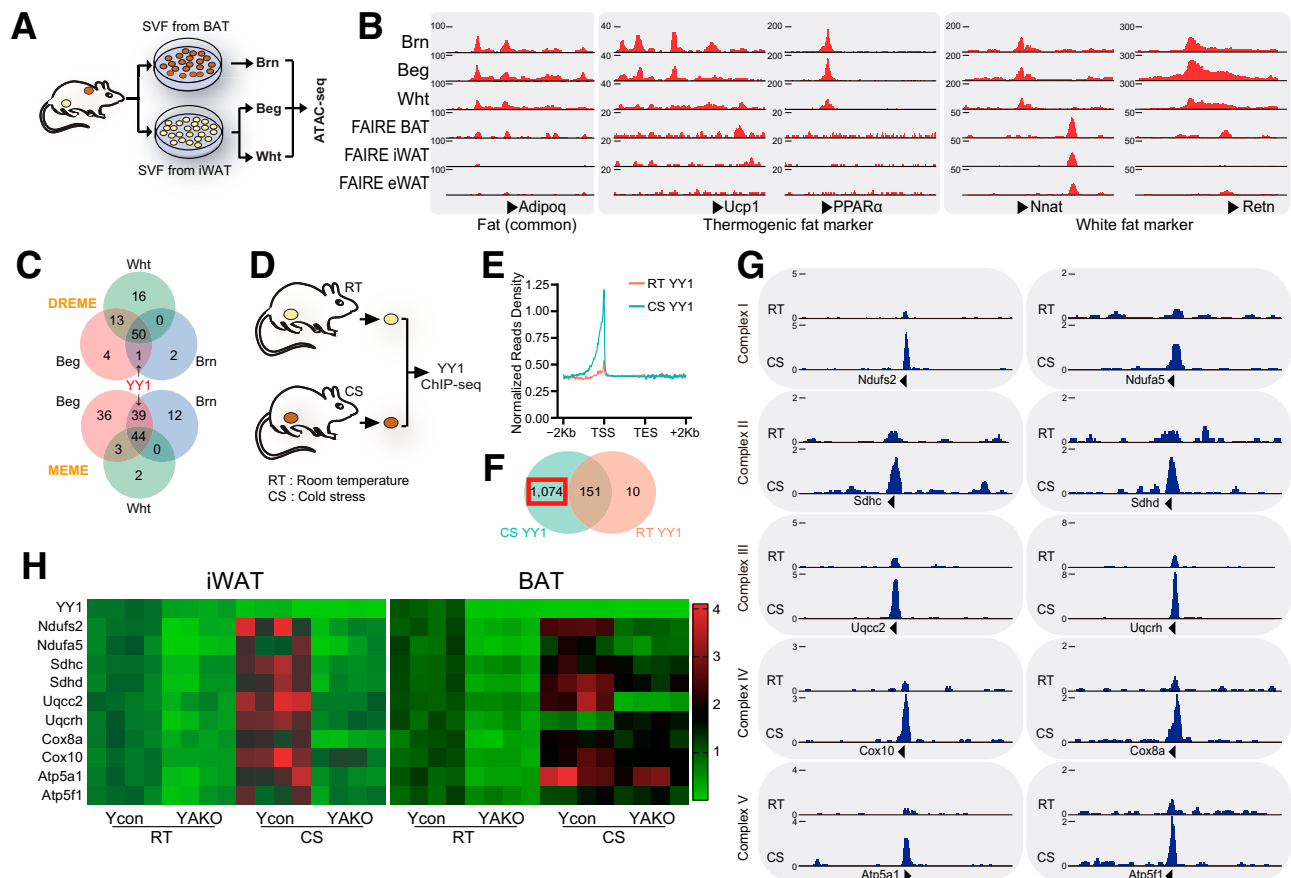


Figure 1—YY1 governs the transcription of mitochondria coding genes in thermogenic adipose. **A–C**: SVFs derived from the BAT and iWAT were collected and cultured in vitro, then induced differentiation into brown (Brn), beige (Beg), and white (Wht) adipocytes, followed by nuclear extraction and ATAC-seq. **A**: Model pattern of the ATAC-seq sample treatment. **B**: The Integrative Genomics Viewer (IGV) tool visualization of the open peaks on the promoter region of adipocyte marker genes. ATAC-seq peaks represent an average of two biological replicates. A published FAIRE-seq data set of BAT, iWAT, and eWAT fat pad (GSE83764) were together analyzed and treated as the control. **C**: De novo motif analysis of the open peaks identified YY1 as a thermogenic adipose-specific DNA binding protein. For each group, an average of two biological replicates were calculated before analysis. **D–G**: Mature adipocytes were separated from iWAT of wild-type C57 mice pretreated with/without 7 days of CS, followed by YY1 ChIP-seq library building and sequencing. **D**: Model pattern of the ChIP-seq sample treatment. **E**: Normalized read count (average of reads signals across all genes) across gene body. **F**: Venn diagram of peaks. **G**: The IGV tool was used to visualize the binding peaks of YY1 on the promoter region of mitochondrial complex coding genes. **H**: Heat map showing the expression of mitochondria coding genes that contains YY1 binding peaks ($n = 4$). YAKO mice ($YY1^{flox/flox};adipoq\text{-}cre$) with their Ycon control littermates ($YY1^{flox/flox}$) were treated with/without a 4°C CS for 7 days, followed by quantitative PCR analysis. Values represent mean \pm SEM.

A comparison with a published Formaldehyde-Assisted Isolation of Regulatory Elements (FAIRE)-seq data set (GSE83764) (9) revealed that our ATAC-seq had more reliable sequencing signals and a lower background (Fig. 1B), thereby providing a useful atlas of open chromatin landscapes for all three types of adipocytes (Supplementary Fig. 1B).

Interestingly, a common adipocyte marker (*adipoq*) and a white adipocyte marker (*Nnat*, *Retn*) had comparable chromatin open states across all three adipocyte types. The observation that the peak signals on the promoters of *Ucp1* and peroxisome proliferator-activated receptor- α (*PPARα*) were much higher in thermogenic adipocytes than in white adipocytes (Fig. 1B) prompted further analysis of these thermogenic-specific open regions. Both the Discriminative Regular Expression Motif Elicitation (DREME)

and the Multiple Em for Motif Elicitation (MEME) analysis identified one candidate, YY1, as a bioactive DNA-binding protein specific to thermogenic adipocytes (Fig. 1C). YY1 is a known transcription factor (10) that was recently found to bind directly to chromatin and promote DNA loop formation (11,12). YY1 was highly enriched in the thermogenic adipocyte open chromatin regions (Supplementary Fig. 1C).

YY1 Promotes the Transcription of ETC Genes During Thermogenesis

YY1 reportedly promotes the transcription of mitochondria-related genes in C2C12 cells (13), β -cells (14), and mesangial cells (15). Chromatin immunoprecipitation assays conducted with high-throughput sequencing (ChIP-seq) for YY1 in adipocytes separated from mice raised at room temperature (RT) or under 4°C cold stress (CS) (Fig. 1D) revealed

enrichment of the binding peak at the ± 1 -kB promoter region of the target genes (Fig. 1E). However, CS enhanced those binding peaks (162 at RT, 1,225 under CS) (Supplementary Fig. 1D), consistent with a pronounced enrichment of YY1 in the thermogenic–open chromatin regions revealed by the ATAC-seq experiments. Kyoto Encyclopedia of Genes and Genomes pathway analysis of the genes near the 1,074 peaks (Fig. 1F) that appeared only in the CS group showed that potential targets involved many mitochondrial coding genes. These could be subcategorized into “oxidative phosphorylation,” “Parkinson disease,” “Huntington disease,” and “Alzheimer disease” (Supplementary Fig. 1E).

Surprisingly, genes coding for all five mitochondria complexes that form the ETC were targets of YY1 (Fig. 1G). In the CS group, the YY1 binding peak on the promoters of these genes was much higher (Fig. 1G), indicating that YY1 may be responsible for the transcriptional regulation of mitochondrial ETC complexes. Indeed, YAKO mice (Supplementary Fig. 1F) showed reduced expression of these ETC coding genes in both iWAT and BAT under both normal and thermogenic conditions (Fig. 1H).

YY1 Is Required for In Vitro Thermogenic Adipogenesis

YY1 also showed in vitro effects on thermogenic adipogenesis. Blocking YY1 decreased the differentiation capacity of beige adipocytes, as reflected by the reduction in lipid droplets stained with Oil Red O (Fig. 2A), as well as

by the lower expression of the thermogenic marker genes (Fig. 2B and C). Seahorse assays showed that YY1-null adipocytes exhibited severe electron transfer disorders, as reflected by reductions in both basal and maximal respiration (Fig. 2D). In brown adipocytes, blocking YY1 led to similar phenotypes (Fig. 2E–H).

Adipocyte YAKO Mice Showed Impaired Thermogenesis Under CS

The YAKO mice were then challenged with CS. No effect on thermogenesis was observed in the YAKO mice at RT (Supplementary Fig. 2A–E); however, when exposed to CS, the YAKO mice showed decreased body temperature (Fig. 3A and B), lower EE (Fig. 3C and D), and reduced VO_2 (Fig. 3E). The CS did not change the food intake (Supplementary Fig. 2F) or respiratory exchange ratio (Supplementary Fig. 2G) in the YAKO mice. The weight of iWAT and epididymal WAT (eWAT) dropped in the YAKO mice in both the CS (Fig. 3F) and the RT (Supplementary Fig. 2H) conditions, indicating that YY1 might also contribute to the differentiation or expansion of adipose tissue. The iWAT and brown adipose tissue (BAT) were also lighter in color after CS in the YAKO mice than in the Ycon littermates (Fig. 3G). Histological staining revealed numerous multilocular lipid droplets in the beige adipocytes of the Ycon mice, whereas the lipid droplets in the YAKO mice remained large and unilocular (Fig. 3H). Consistent reductions were observed in the expression of thermogenic marker genes (Fig. 3I–J) in both

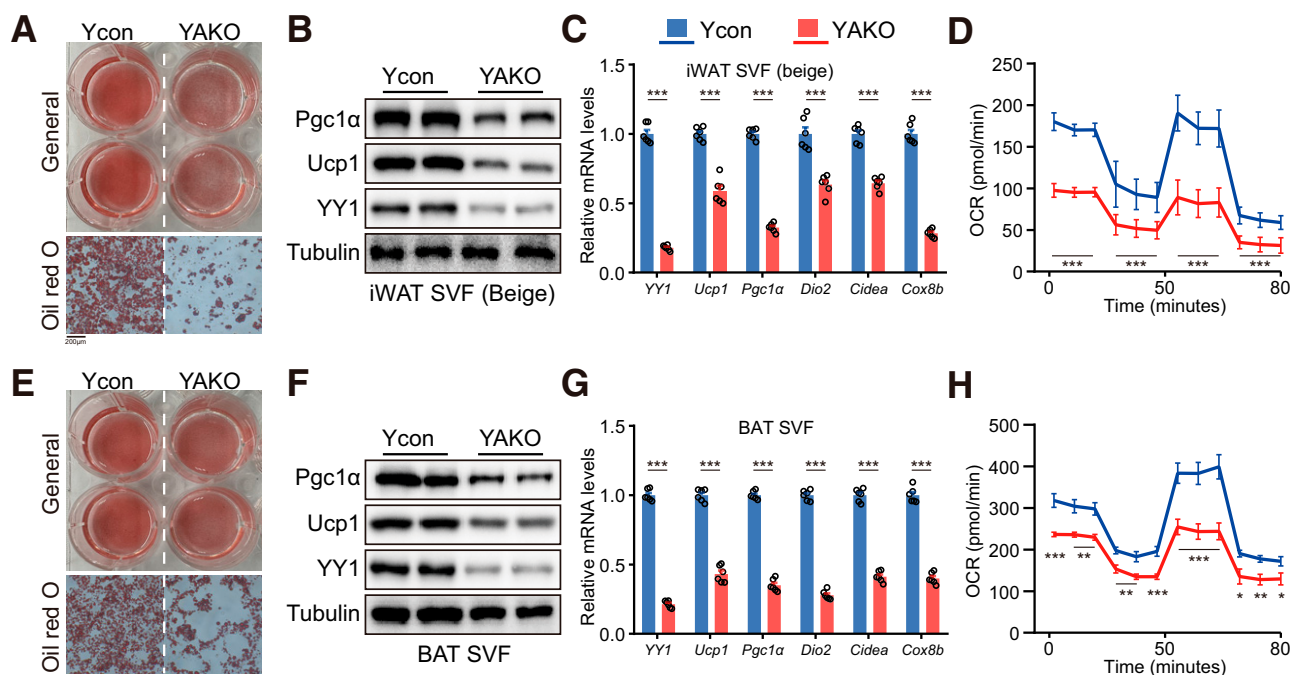


Figure 2—YY1 is necessary for thermogenic adipogenesis and cellular respiration in vitro. SVFs separated from iWAT (A–D) or BAT (E–H) of Ycon or YAKO were differentiated into beige and brown adipocytes, respectively. A and E: Oil Red O staining of lipid droplets ($n = 2$). Scale bar: 200 μm . B and F: Western blot assay testing the protein levels of YY1, Pgc1 α , and Ucp1 ($n = 2$). C and G: Quantitative PCR analyzing the expression of YY1 and thermogenic marker genes ($n = 6$). D and H: Oxygen consumption rate (OCR) measured by Seahorse assay ($n = 8$). Values represent mean \pm SEM. * $P < 0.05$, ** $P < 0.01$, *** $P < 0.001$.

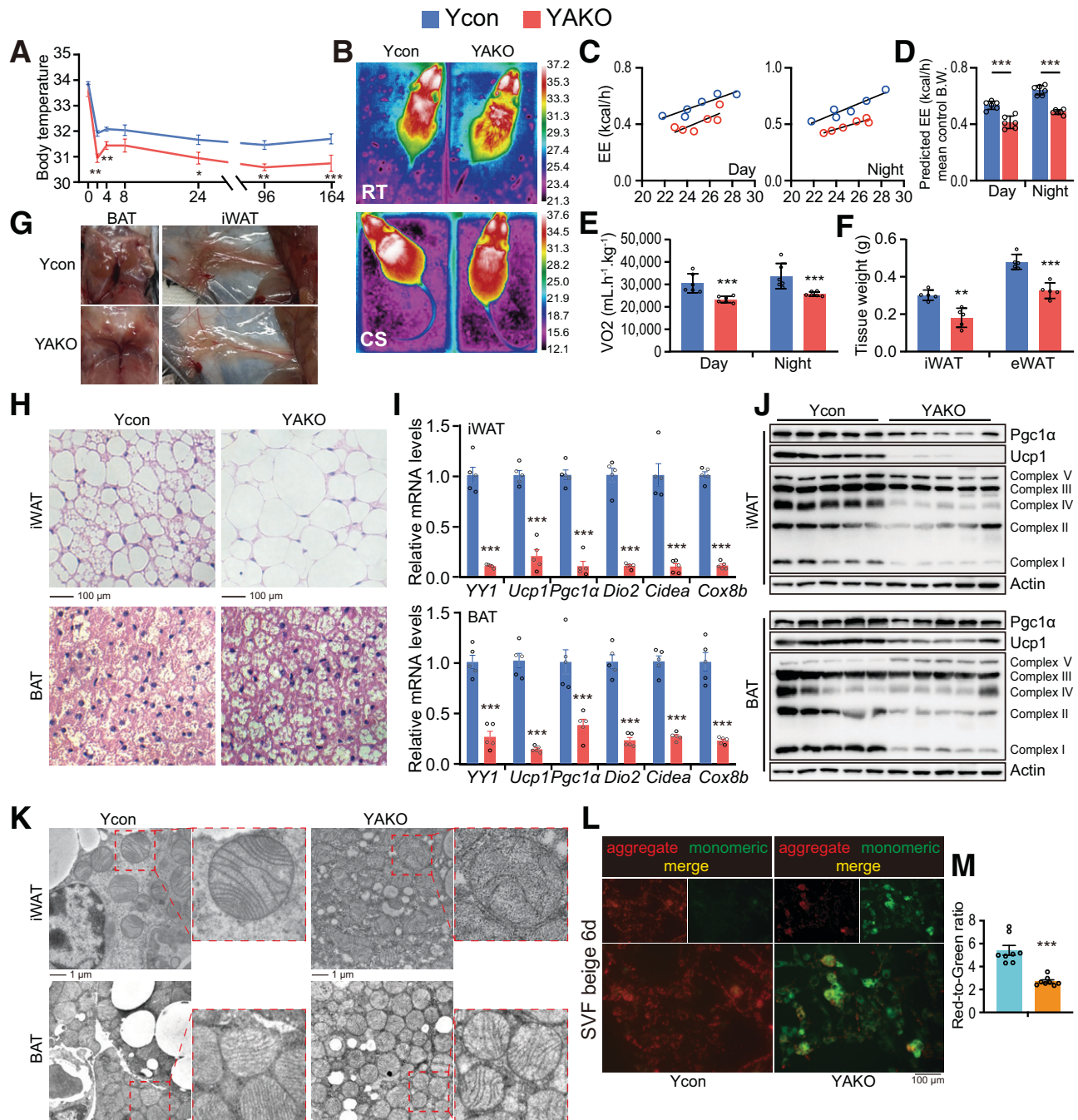


Figure 3—Adipocyte YY1 governs mitochondria function and is necessary for thermogenic activation. A–K: YAKO and Ycon mice were treated with a 4°C CS for 7 days. A: Rectal temperature during CS assay ($n = 5$ for each group). B: Infrared image showing the body temperature before and after CS. C–E: On day 7, the CS mice were transferred to the home cage system, and metabolic parameters from day 8 to day 9 were analyzed ($n = 5$ for each group). C: Regression plots of EE against body weight. D: Predicted EE at the mean body weight of Ycon mice (25.0 g). E: VO_2 level. F–K: On day 7, the CS mice were sacrificed and analyzed ($n = 5$ for each group). F: Tissue weight of fat pads. G: General morphology of BAT and iWAT of the mice. H: Hematoxylin and eosin staining of iWAT and BAT. Scale bar: 100 μ m. I: Quantitative PCR testing YY1, and thermogenic fat marker genes. J: Immunoblot testing Ucp1, Pgc1 α , and mitochondria complex. K: Transmission electron microscopy showing the structure of mitochondria. L and M: SVF cells separated from iWAT of Ycon or YAKO mice were differentiated into beige adipocytes, followed by JC-1-mediated mitochondrial membrane potential (MMP) analysis. L: Image of JC-1 fluorescence. Red fluorescence represents the mitochondrial aggregate JC-1, and green fluorescence indicates the monomeric JC-1. M: Graph represents the ratio of aggregated and monomeric JC-1, measured by dual-emission fluorescence microplate reader ($n = 8$ for each group). Values represent mean \pm SEM. * $P < 0.05$, ** $P < 0.01$, *** $P < 0.001$.

the iWAT and the BAT of the YAKO mice, indicating thermogenic impairment.

Local Blockage of YY1 in Subcutaneous Fat Impairs, Rather Than Enhances, the Beiging Process

A previous study showed that Ucp1-cre-mediated YY1 deletion impairs BAT function but somehow promotes beige adipogenesis (16). To clarify the precise regulatory effect of YY1 on the beiging of subcutaneous adipose tissue and exclude the potential impact of continuous YY1 KO on the differentiation and enlargement of the fat pad (Fig. 3F and Supplementary Fig. 2H), local AAV8-mediated YY1 knockdown was performed in iWAT (Supplementary Fig. 2I). As was seen in YAKO mice, this local blocking of YY1 in iWAT obstructed CS-induced beige activation (Supplementary Fig. 2J and K), while also reducing the expression of thermogenic markers after CS (Supplementary Fig. 2L and M). As expected, subcutaneous AAV injection did not affect the expression of YY1 in BAT or alter the thermogenic activation of brown adipocytes subjected to CS (Supplementary Fig. 2J–M).

YY1 Is Required for the Maintenance of ETC Function and Mitochondrial Membrane Potential in Thermogenic Adipocytes

Because YY1 was found to govern the transcription of ETC genes, we investigated whether the loss of YY1 affected mitochondrial morphology and function. Transmission electron microscopy analysis of the mitochondrial ultrastructure revealed that YAKO adipocytes had a significant reduction in cristae, the site at which the ETC complex is assembled (Fig. 3K). The YAKO adipocytes also showed a consistently reduced expression of mitochondrial complexes I–IV (Fig. 3J), as well as a lower mitochondrial membrane potential (Fig. 3L and M), which is generated by the proton pump activity of complexes I, III, and IV. The importance of YY1 in the maintenance of mitochondrial function was further confirmed in AAV-induced YAKO mice (Supplementary Fig. 2F).

YY1 Deficiency Protects Mice From Diet-Induced Obesity and Metabolic Syndrome

Challenging the YAKO mice with diet-induced obesity revealed the interesting observation that despite decreased expression of thermogenic marker and ETC complex proteins (Supplementary Fig. 3A), the YAKO mice were resistant to diet-induced obesity (Fig. 4A and Supplementary Fig. 3B), consistent with a previous study (16). The YAKO mice also showed reduced blood glucose levels (Fig. 4B), together with enhanced glucose and insulin tolerance (Fig. 4C and D). Metabolic cage assay results suggested that although the food intake was comparable (Supplementary Fig. 3C), the YAKO mice had a higher EE at night (Supplementary Fig. 3D and E) and locomotor activity (Supplementary Fig. 3F), which could combat obesity. Analysis of the fat pad revealed a sharp decrease in adipose tissue weight in the YAKO mice (Fig. 4E and Supplementary Fig. 3G). Although BAT whitening was enhanced, the iWAT and eWAT in YAKO mice showed far fewer inflammatory cells

and crown-like structures (CLS) compared with the Ycon mice (Fig. 4F and G), suggesting a reduction in adipose tissue inflammation in the YAKO mice. No alleviation was observed in liver steatosis (Supplementary Fig. 3H and I) or insulin resistance (Supplementary Fig. 3J).

The adipose tissue macrophages (ATMs) are regarded as the primary contributors to adipose tissue inflammation and insulin resistance (17,18). Macrophage infiltration and inflammatory responses in the iWAT and eWAT were reduced in YAKO mice, and the insulin sensitivity of the fat pads was significantly increased (Fig. 4H). Interestingly, the insulin sensitivity of BAT did not improve (Fig. 4H). The differences in the distribution of ATMs in the fat pad, with more ATMs in eWAT and iWAT than in BAT (19), correlated with the observed changes in insulin sensitivity, suggesting that macrophages may mediate the metabolic improvement seen in YAKO mice.

YAKO Mice Show Promotion of ATM M2 Polarization

Flow cytometry (Supplementary Fig. 4) analysis revealed that, compared with Ycon mice, YAKO mice had ~88% fewer macrophages in iWAT and ~73% fewer in eWAT, but a comparable number in BAT (Fig. 5A–C). These findings were consistent with the F4/80 staining results (Fig. 4G). The YAKO mice also showed lower numbers of proinflammatory M1-like macrophages (Fig. 5D and E) and higher numbers of alternative M2-like macrophages (Fig. 5G and H), whereas the ATM numbers in BAT were unchanged (Fig. 5F and I). Taken together, these data suggested that HFD-induced ATM M1 polarization was ameliorated in the white fat pad of the YAKO mice.

YY1-Deficient Adipocytes Undergo Metabolic Reprogramming

As key endocrine cells, adipocytes reportedly affect the activities of nearby ATMs by secreting signaling molecules, including metabolites (20,21). Metabolomics analysis revealed that YY1 deficiency rewired adipocyte metabolism, leading to increased levels of lactate, succinate, fumarate, and malate (Fig. 6A). Interestingly, despite the impairment of the ETC in YY1-null adipocytes, the cells had similar adenylate energy charges (Fig. 6A). This could reflect enhanced glycolysis activity in the YY1-null cells, as indicated by the increased lactate level (Fig. 6A). The NAD^+ -to-NADH ratio was also higher in the YY1-null adipocytes than in the control cells (Fig. 6B), indicating a decrease in the hydrogen supply from TCA mediators.

The activation of glycolysis and the inhibition of the TCA cycle in YY1-deficient adipocytes were confirmed using stable isotopic tracer-based metabolic flux analysis (Fig. 6C). The $[\text{U-}^{13}\text{C}]$ glucose tracer assay showed that blocking YY1 in adipocytes raised the m +3 lactate content and reduced the m +2 citrate, m +2 α -ketoglutarate (α KG), m +2 succinate, and m +2 fumarate contents (Fig. 6D), suggesting a rewiring of glucose metabolism in YAKO adipocytes toward lactate and away from the TCA

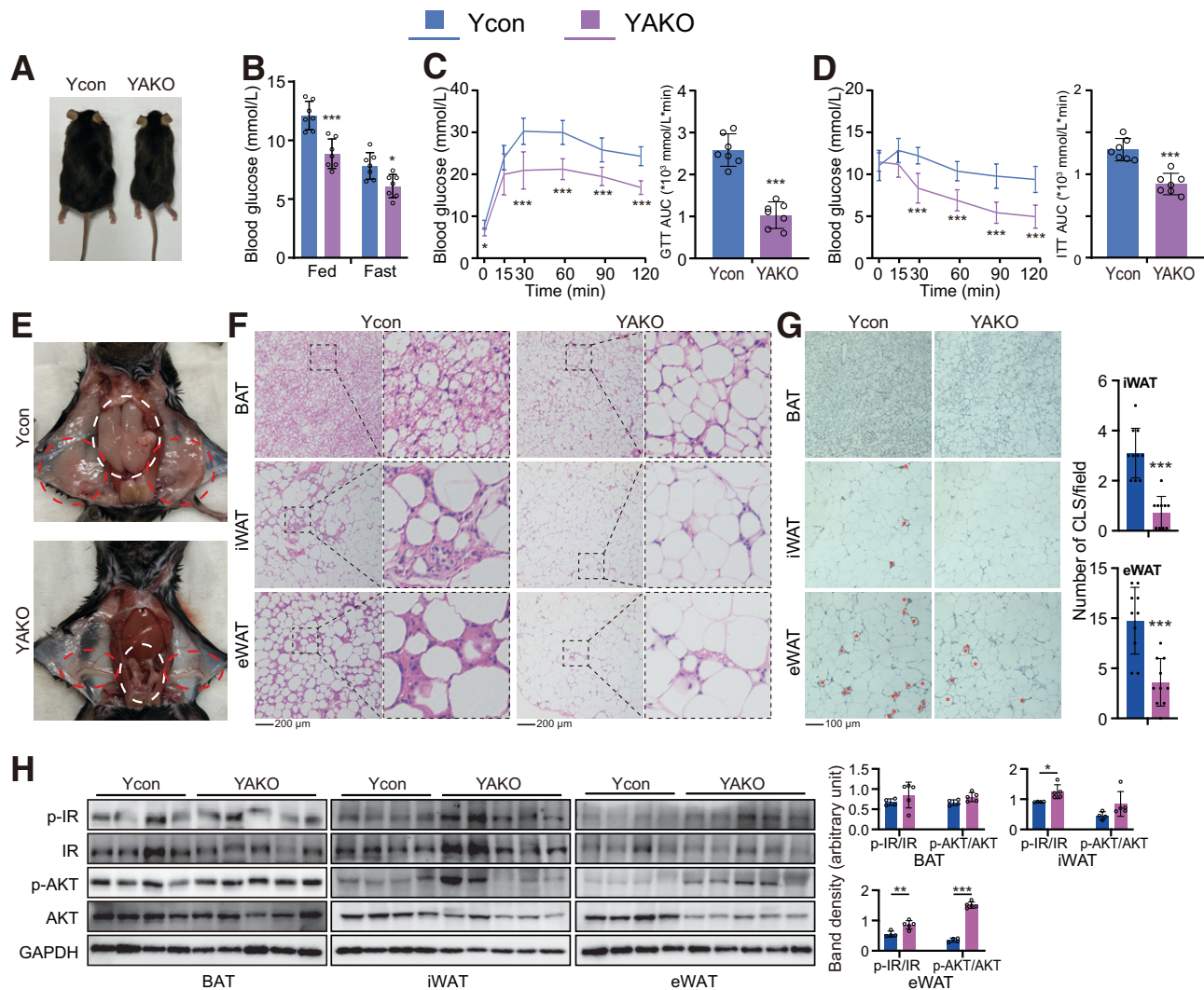


Figure 4—Adipocyte YY1 deficiency protects mice from diet-induced obesity and insulin resistance. A–G: YAKO and Ycon mice at the age of 4–5 weeks were fed a HFD for 16 weeks before analysis ($n = 7$ for each group). A: General morphology of the mouse bodies. B: The random and fasting (14 h) blood glucose levels. C: Glucose tolerance test (GTT) assay (left) and the calculated area under the curve (AUC) of GTT (right). D: Insulin tolerance test (ITT) assay (left) and the calculated AUC of ITT (right). E: General image of the WAT. Red circle, iWAT; white circle, eWAT. F: Hematoxylin and eosin staining of adipose tissue sections. G: F4/80 immunohistochemical staining of adipose tissue sections (left). Red asterisk, CLS. In each group, the CLS were calculated from 10 photographs obtained from 5 mice (right). H: Western blot assays (left) testing insulin sensitivity in all three fat pads of Ycon and YAKO mice. The HFD was fed to another batch of mice for 16 weeks. After a 4-h fast, Ycon ($n = 4$) and YAKO ($n = 5$) were injected i.p. with 5 units/kg insulin and sacrificed 10 min later. Right, calculated arbitrary unit of phosphorylated (p) insulin receptor (p-IR)/IR, and p-AKT/AKT. Values represent mean \pm SEM. * $P < 0.05$, ** $P < 0.01$, *** $P < 0.001$.

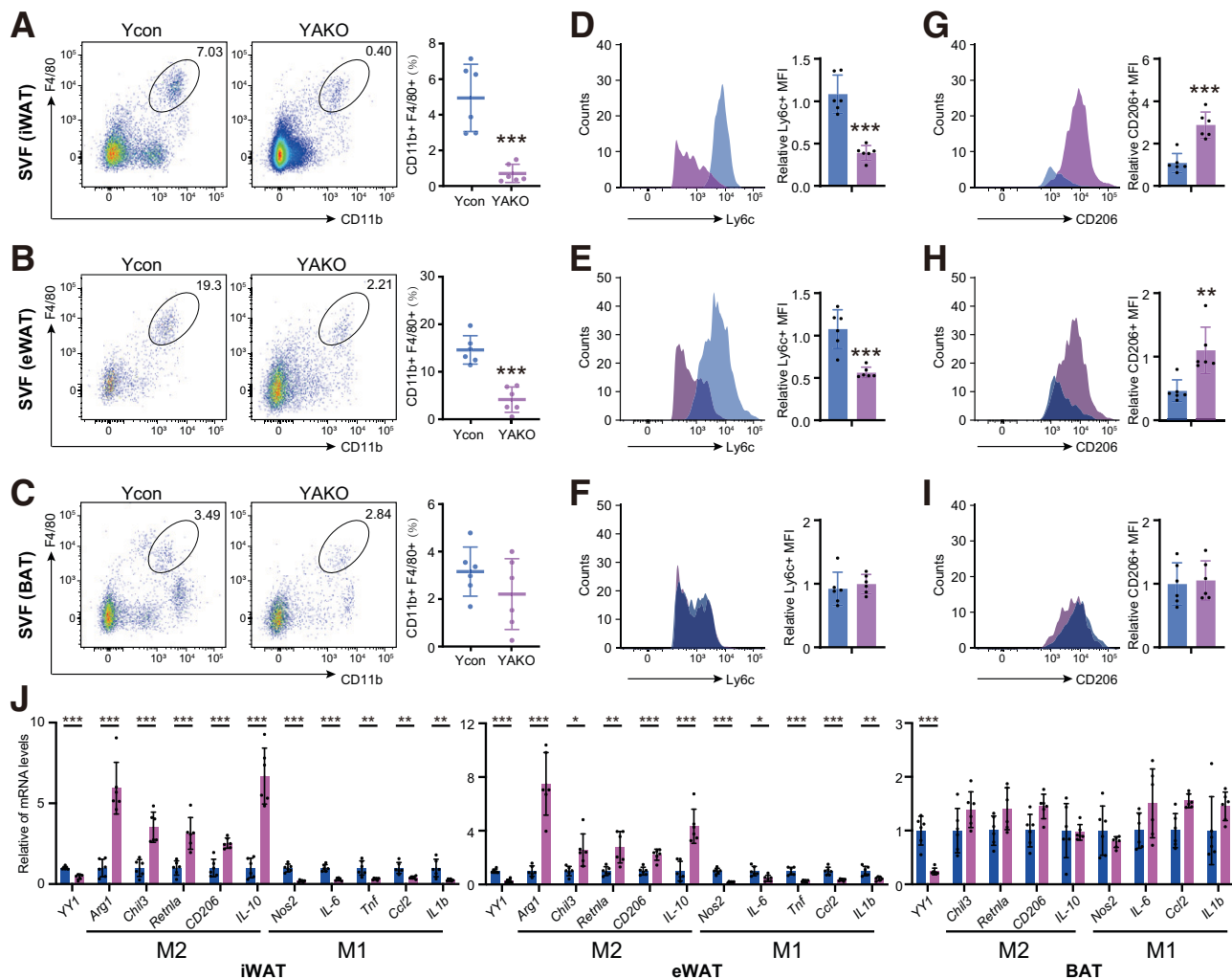
cycle. However, the intermediate TCA cycle metabolites did not decrease in YAKO adipocytes (Fig. 6A), indicating that YAKO adipocytes use metabolites other than glucose to replenish the TCA cycle.

Further assessment revealed that YY1-deficient adipocytes showed enhanced glutamine use, as confirmed by [$^{13}\text{C}_5$]glutamine metabolism assays. The increased m +5 α KG content in YAKO adipocytes indicated that a large amount of glutamine underwent deamination, while the increase in m +4 succinate, m +4 fumarate, and m +4 citrate content indicated that the glutamine carbon skeleton entered the TCA cycle (Fig. 6E). Interestingly, an increase in m +5 citrate also occurred, indicating that

blocking YY1 may enhance the reductive carboxylation pathway in adipocytes (Fig. 6E). In summary, YY1-deficient adipocytes showed enhanced glutamine fluxes in both the forward and reverse directions, suggesting that glutamine functions as an anaplerotic source for the TCA cycle.

YY1-Null Adipocytes Generate Spd and Promote Macrophage M2 Polarization

For glutamine to serve as an anaplerotic source for the TCA cycle, it must first participate in deamination or transamination reactions (22). Consistent with the enhanced glutamine use observed in YY1-null adipocytes, we also noted an increase in arginine-succinate and ornithine content,



indicating activation of the urea cycle (Fig. 6A). In addition to citrulline, ornithine can be converted into putrescine to generate anti-inflammatory polyamines, such as Spd (23). Accordingly, knocking out YY1 in adipocytes increased the expression of ornithine decarboxylase 1 (Odc1), the rate-limiting enzyme that governs the decarboxylation of ornithine to form putrescine (Fig. 7A).

Spd can be imported into macrophages (24), where it modulates the activation of M2 macrophages (25). This macrophage activation, in turn, reduces adipose tissue inflammation and lowers the fat mass in HFD-induced obese mice (26). Blocking Odc1 expression by in situ injection of sh-AAV into the iWAT of YAKO mice reduced the Spd content (Fig. 7B). Local blocking of Odc1 showed no effect on blood glucose levels (Fig. 7C), yet slightly

reversed the protective effect of YAKO on body weight (Fig. 7D and E), glucose clearance capacity (Fig. 7F), and insulin sensitivity (Fig. 7G). In iWAT, blocking Odc1 significantly reversed the protective effect of YAKO on the iWAT tissue weight (Fig. 7H), inflammation (Fig. 7I–J), and insulin signaling transduction (Fig. 7K), as well as macrophage M2 polarization (Fig. 7L).

The adipocyte-macrophage communication mediated by Odc1-Spd was also confirmed using conditioned medium (CDM) culture. CDM from YY1-null adipocytes blocked the inflammatory activation of macrophages and activated an alternative M2 polarization (Fig. 7M). Blocking the Odc1 enzyme activity in adipocytes with eflornithine, an irreversible inhibitor, reversed this effect (Fig. 7M). Blocking the organic cation transporters (OCT 1/2/3; also known as

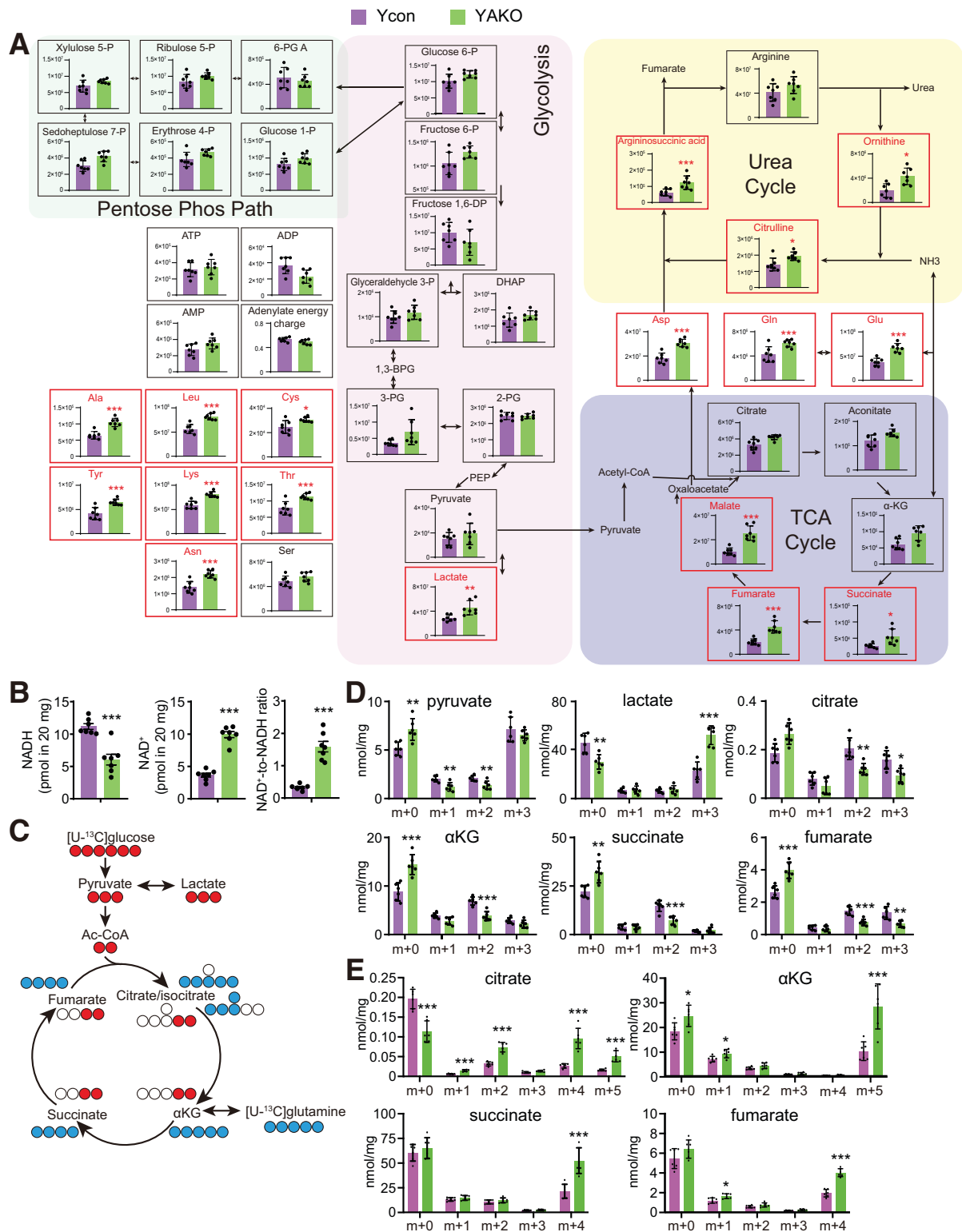


Figure 6—Adipocyte YY1 deficiency rewires glucose metabolism and enhances glutamine use. SVFs separated from iWAT of Ycon or YAKO were differentiated into white adipocytes. **A** and **B**: Targeted metabolomics of adipocyte were performed ($n = 7$). **A**: Each bar chart represents the content of a metabolite. The bar charts are displayed alongside the metabolic transformation centered with glycolysis, TCA cycle, urea cycle, and pentose phosphate pathways. 2-PG, 2-phosphoglycerate; 3-PG, 3-phosphoglyceric acid; DHAP, dihydroxyacetone phosphate. **B**: NADH, NAD⁺ content, and the NAD⁺-to-NADH ratio. **C–E**: Stable isotope-based metabolic flux assay of adipocytes was performed ($n = 6$). **C**: Schematic of labeled glucose or glutamine fluxes into the TCA cycle. The content of the [U-¹³C] isotopologue of indicated metabolites in [U-¹³C]glucose assay (**D**) and [U-¹³C]glutamine assay (**E**). Values represent mean \pm SEM. * $P < 0.05$, ** $P < 0.01$, *** $P < 0.001$.

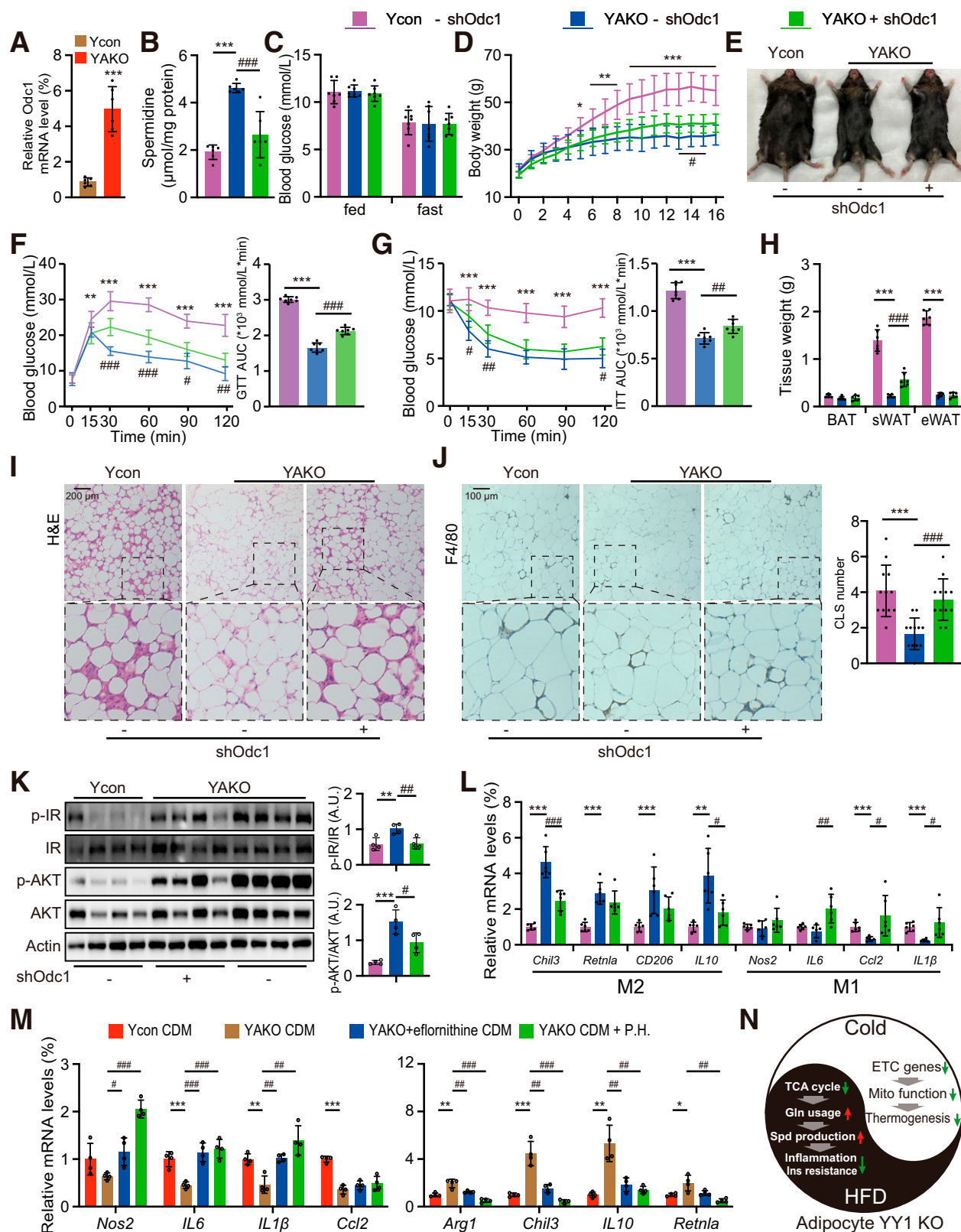


Figure 7—YY1-null adipocytes generate Spd and promote macrophage M2 polarization. **A**: Quantitative PCR analyses of *Odc1*. YAKO and Ycon mice at the age of 4–5 weeks were fed the HFD for 14 weeks before analysis ($n = 6$ for each group). **B–L**: YAKO ($n = 12$) and Ycon ($n = 6$) mice at the age of 4–5 weeks were fed the HFD. After 2 weeks, the Ycon mice and half of the YAKO mice ($n = 6$) were injected with noncoding (NC)-AAV, while the other half of the YAKO mice ($n = 6$) were injected with sh-*Odc1* AAV into iWAT. The mice continued to be fed the HFD for another 14 weeks (16 weeks total). **B**: Spd content of the iWAT. **C**: The random and fasting (14 h) blood glucose levels. **D**: Body weight. **E**: General morphology of the mouse bodies. **F**: Glucose tolerance test (GTT) assay (left) and the calculated area under the curve (AUC) of GTT (right). **G**: Insulin tolerance test (ITT) assay (left) and the calculated AUC of ITT (right). **H**: Fat pad tissue weight.

SLC22A1/2/3 [27]) required for the entry of positively charged Spd into cells with an OCT inhibitor can also reverse the protective effect of YAKO (Fig. 7M). Taken together, these findings revealed that YY1-null adipocytes activate the Odc1-Spd axis to communicate with macrophages and promote M2 polarization.

DISCUSSION

Thermogenic adipose tissue is believed to protect the body from obesity and metabolic disorders, and an enduring consensus has been that reductions in mitochondrial mass and/or function in thermogenic adipose tissues sabotage this protective function. However, recent studies have suggested that the metabolic benefits provided by thermogenic adipose tissue do not depend solely on an increase in mitochondrial numbers. Several rodent-based studies have unexpectedly revealed that blocking specific signals that play key roles in maintaining mitochondrial function can reduce the thermogenic function of adipose tissues, and yet the rodents remain protected from HFD-induced metabolic disorders (5–7). Several hypotheses have been proposed to explain the mechanism of how the body may benefit from HFD feeding, even in the presence of thermogenic adipose tissue dysfunction, such as ETC proteome imbalance triggering mitochondrial unfolded protein response and inducing metabolic fitness (5), promoting the clearance of peripheral lipids by activating lipoprotein lipase and CD36 (6) or the mtDNA/NLRP3 inflammasome pathway (7). At present, however, the precise mechanism and functional impact of the uncoupling of thermogenic capacity and metabolic benefits remain unexplored.

Our profiling of the open chromatin atlas of white, beige, and brown adipocytes identified YY1 as a key governor of mitochondrial function. Interestingly, the disconnection between thermogenic capacity and beneficial metabolic changes in YAKO mice appeared to be a result of reduced inflammation (Fig. 7N). In the absence of YY1, adipocytes with impaired mitochondrial function underwent metabolic reprogramming to generate Spd, which inhibited the proinflammatory M1 polarization of macrophages and thereby alleviated HFD-related adipose tissue inflammation. This result, consistent with the findings of previous studies (5–7,28), suggests that a distinction should be made regarding thermogenic activation and the metabolic benefits currently attributed to adipose tissue. Moreover, the coordinating role of

mitochondria as mediators of thermogenesis and beneficial metabolism should also be carefully evaluated.

Many studies have identified that a key function of YY1 is to maintain proper mitochondrial function. Consistently, our data suggest that YY1 KO alters the morphology and function of mitochondria and reduces thermogenesis. However, another study reported that YY1 KO mediated by Ucp1-cre enhanced iWAT browning (16). Our AAV-mediated blockage of YY1 in vivo assays, as well as primary adipocyte-based in vitro assays, clearly illustrated the inhibitory effect of blocking YY1 on the differentiation and thermogenic capacity of beige fat. Interestingly, we did find some consistency between our results and those of the previous study (16); that is, although YAKO mice showed suppressed brown fat activity, the metabolic disorders in subcutaneous fat were alleviated.

Interestingly, the YAKO mice showed a decrease in EE under CS, but their EE increased under HFD feeding, which could explain their antiobesity phenotype. While the food intake was comparable, we noticed that the EE was much higher in the YAKO mice after HFD feeding. Notably, regression-based analysis of the EE data using ANCOVA (29) to eliminate the potential influence of body size variation in the group comparisons showed that the EE was still higher in the YAKO mice. Consistent with this, the changes in EE of YAKO mice were already evident as soon as 2 weeks after the HFD was initiated, when the body weights between the control and mutant mice were still comparable (16). The YAKO mice showed a more severe whitening of BAT after HFD feeding, suggesting that the thermogenic effect contributed relatively little to the increased EE. An interesting point worth mentioning is that YAKO mice have a higher EE during the night (the normal active state for mice). The higher locomotory activity of the YAKO mice suggests the possibility that they expend more energy in physical activity. In addition, the upregulation of the Odc1-Spd pathway in YAKO mice may also be involved in combating obesity, as heterozygous KO of Odc1 in *Drosophila* (homozygous lethal) leads to fat accumulation and weight gain (30), whereas supplementation with Spd activates mitochondrial respiration (31) and raises EE.

As key endocrine cells, adipocytes reportedly affect the nearby ATM activity by secreting signaling molecules, such as metabolites (20,21), cytokines (32,33), extracellular

I: Hematoxylin and eosin (H&E) staining of adipose tissue sections. J: F4/80 immunohistochemical staining of adipose tissue sections (left). In each group, the CLS were calculated from 12 photographs obtained from 6 mice (right). K: Left: Western blot assays testing insulin sensitivity in iWAT of Ycon and YAKO mice. After a 4-h fasting, mice were injected i.p. with 5 units/kg insulin and sacrificed 10 min later. Right: Calculated arbitrary unit of phosphorylated (p) insulin receptor (p-IR)/IR, and p-AKT/AKT. L: Quantitative PCR analyses of the mRNA abundance of the indicated genes. M: Bone marrow-derived macrophages were treated with 50% adipocyte conditional medium (CDM) for 24 h before qPCR testing the expression of M1 (left) and M2 (right) marker genes. SVF-derived control or YY1-null white adipocytes (4 days after differentiation) were cultured to collect CDM. For Odc1 blockage, 250 $\mu\text{mol/L}$ eflornithine was added into adipocyte during differentiation (before CDM collection). For organic cation transporters blockage, 20 $\mu\text{mol/L}$ prazosin hydrochloride (P.H.) was added directly into CDM. N: Graphic abstract. Values represent mean \pm SEM. For Ycon vs. YAKO, Ycon-shOdc1 vs. YAKO -shOdc1, and Ycon CDM vs. YAKO CDM: * $P < 0.05$, ** $P < 0.01$, *** $P < 0.001$. For YAKOshOdc1 vs. YAKO+shOdc1, YAKO CDM vs. YAKO+eflornithine, and YAKO CDM vs. YAKO CDM+P.H.: # $P < 0.05$, ## $P < 0.01$, ### $P < 0.001$.

vesicles (34,35), or even cellular organelles (36,37). Our metabolomics analysis revealed that YY1 knockdown activates glycolysis, glutamine uptake, and the generation of anti-inflammatory Spd. Another question arises from our metabolic flux and the NAD⁺-to-NADH ratio data, which suggest that the TCA cycle is blocked in YAKO adipocytes. Therefore, where do the increased succinate, fumarate, and malate come from? We speculate that two sources are available: 1) YAKO adipocytes ingest more glutamine, which is deaminated into α KG and then converted into succinate, or 2) YAKO adipocytes have higher urea cycle activity that breaks down argininosuccinic acid to produce fumarate for the TCA. Notably, increasing evidence suggests that adipocytes, and especially thermogenic adipocytes, can consume large amounts of amino acids, such as branched chain amino acids (28,38). One possibility is that thermogenic adipocytes have a high capacity for amino acid catabolism, similar to that occurring in the liver. This idea is supported by recent studies that have identified an intact urea cycle in thermogenic adipocytes (39,40).

Collectively, the findings of this study represent a major step toward understanding the uncoupling of thermogenic capacity and beneficial metabolism. Our study has identified an essential mediator, Spd, as a link between mitochondrial dysfunction and the alleviation of inflammation in thermogenic adipose tissue.

Funding. This research was funded by grants from the National Natural Science Foundation of China (82070897 and 32471172 to K.L., 82472393 to Q.Z., and 82000735 to K.W.) and by Key Research Project of Taizhou School of Clinical Medicine, Nanjing Medical University (TZKY20230307 to K.L. and S.Y.). This work was also supported by the Taizhou Basic Public Health Service Application Research Project (TPH202204 to S.Y.), by the Taizhou People's Hospital Hospital-level Scientific Research Fund Project (ZL202219 to S.Y.), and by the Natural Science Foundation of Jiangsu Province, China (BK20200118 to K.W.).

Duality of Interest. No potential conflicts of interest relevant to this article were reported.

Author Contributions. C.Q., Y.L., and S.W. performed experiments. C.Q., P.S., and K.L. analyzed data and wrote the manuscript. W.G., J.N., J.S., Z.L., X.C., and K.W. assisted in completing part of the experiments. Q.Z., S.Y., and K.L. designed the study and provided guidance. All authors reviewed, edited, and approved the manuscript. K.L. is the guarantor of this work and, as such, had full access to all the data in the study and takes responsibility for the integrity of the data and the accuracy of the data analysis.

References

- Lowell BB, S-Susulic V, Hamann A, et al. Development of obesity in transgenic mice after genetic ablation of brown adipose tissue. *Nature* 1993;366:740–742
- Betz MJ, Enerbäck S. Targeting thermogenesis in brown fat and muscle to treat obesity and metabolic disease. *Nat Rev Endocrinol* 2018;14:77–87
- Chouchani ET, Kazak L, Spiegelman BM. New advances in adaptive thermogenesis: UCP1 and beyond. *Cell Metab* 2019;29:27–37
- Cohen P, Kajimura S. The cellular and functional complexity of thermogenic fat. *Nat Rev Mol Cell Biol* 2021;22:393–409
- Masand R, Paulo E, Wu D, et al. Proteome imbalance of mitochondrial electron transport chain in brown adipocytes leads to metabolic benefits. *Cell Metab* 2018;27:616–629.e614
- Mahdavi K, Benador IY, Su S, et al. Mfn2 deletion in brown adipose tissue protects from insulin resistance and impairs thermogenesis. *EMBO Rep* 2017;18:1123–1138
- Huang Y, Zhou JH, Zhang H, et al. Brown adipose TRX2 deficiency activates mtDNA-NLRP3 to impair thermogenesis and protect against diet-induced insulin resistance. *J Clin Invest* 2022;132
- Lu Y, Ma Z, Zhang Z, et al. Yin Yang 1 promotes hepatic steatosis through repression of farnesoid X receptor in obese mice. *Gut* 2014;63:170–178
- Hiraike Y, Waki H, Yu J, et al. NFIA co-localizes with PPAR γ and transcriptionally controls the brown fat gene program. *Nat Cell Biol* 2017;19:1081–1092
- Shi Y, Seto E, Chang LS, Shenk T. Transcriptional repression by YY1, a human GLI-Krüppel-related protein, and relief of repression by adenovirus E1A protein. *Cell* 1991;67:377–388
- Li L, Williams P, Ren W, et al. YY1 interacts with guanine quadruplexes to regulate DNA looping and gene expression. *Nat Chem Biol* 2021;17:161–168
- Weintraub AS, Li CH, Zamudio AV, et al. YY1 is a structural regulator of enhancer-promoter loops. *Cell* 2017;171:1573–1588.e28
- Cunningham JT, Rodgers JT, Arlow DH, Vazquez F, Mootha VK, Puigserver P. mTOR controls mitochondrial oxidative function through a YY1-PGC-1 α transcriptional complex. *Nature* 2007;450:736–740
- Song D, Yang Q, Jiang X, et al. YY1 deficiency in β -cells leads to mitochondrial dysfunction and diabetes in mice. *Metabolism* 2020;112:154353
- Gao P, Li L, Yang L, et al. Yin Yang 1 protein ameliorates diabetic nephropathy pathology through transcriptional repression of TGF β 1. *Sci Transl Med* 2019;11:eaaw2050
- Verdeguer F, Soustek MS, Hatting M, et al. Brown adipose YY1 deficiency activates expression of secreted proteins linked to energy expenditure and prevents diet-induced obesity. *Mol Cell Biol* 2015;36:184–196
- Johnson AMF, Olefsky JM. The origins and drivers of insulin resistance. *Cell* 2013;152:673–684
- Weisberg SP, McCann D, Desai M, Rosenbaum M, Leibel RL, Ferrante AW Jr. Obesity is associated with macrophage accumulation in adipose tissue. *J Clin Invest* 2003;112:1796–1808
- Villena JA, Cousin B, Pénicaud L, Casteilla L. Adipose tissues display differential phagocytic and microbicidal activities depending on their localization. *Int J Obes Relat Metab Disord* 2001;25:1275–1280
- Feng T, Zhao X, Gu P, et al. Adipocyte-derived lactate is a signalling metabolite that potentiates adipose macrophage inflammation via targeting PHD2. *Nat Commun* 2022;13:5208
- Petrus P, Lecoutre S, Dollet L, et al. Glutamine links obesity to inflammation in human white adipose tissue. *Cell Metab* 2020;31:375–390.e311
- DeNicola GM, Cantley LC. Cancer's fuel choice: new flavors for a picky eater. *Mol Cell* 2015;60:514–523
- Madeo F, Eisenberg T, Pietrocola F, Kroemer G. Spermidine in health and disease. *Science* 2018;359:eaan2788
- McCubrey AL, McManus SA, McClendon JD, et al. Polyamine import and accumulation causes immunomodulation in macrophages engulfing apoptotic cells. *Cell Rep* 2022;38:110222
- Puleston DJ, Buck MD, Klein Geltink RI, et al. Polyamines and eIF5A hypusination modulate mitochondrial respiration and macrophage activation. *Cell Metab* 2019;30:352–363.e8
- Ma L, Ni Y, Hu L, et al. Spermidine ameliorates high-fat diet-induced hepatic steatosis and adipose tissue inflammation in preexisting obese mice. *Life Sci* 2021;265:118739
- Sala-Rabanal M, Li DC, Dake GR, et al. Polyamine transport by the polyspecific organic cation transporters OCT1, OCT2, and OCT3. *Mol Pharm* 2013;10:1450–1458
- Verkerke ARP, Wang D, Yoshida N, et al. BCAA-nitrogen flux in brown fat controls metabolic health independent of thermogenesis. *Cell* 2024;187:2359–2374.e18
- Kaijala KJ, Morton GJ, Leroux BG, Ogimoto K, Wisse B, Schwartz MW. Identification of body fat mass as a major determinant of metabolic rate in mice. *Diabetes* 2010;59:1657–1666

30. Leon KE, Fruin AM, Nowotarski SL, DiAngelo JR. The regulation of triglyceride storage by ornithine decarboxylase (Odc1) in *Drosophila*. *Biochem Biophys Res Commun* 2020;523:429–433
31. Schroeder S, Hofer SJ, Zimmermann A, et al. Dietary spermidine improves cognitive function. *Cell Rep* 2021;35:108985
32. Choi CHJ, Barr W, Zaman S, et al. LRG1 is an adipokine that promotes insulin sensitivity and suppresses inflammation. *Elife* 2022;11:e81559
33. Funcke J-B, Scherer PE. Beyond adiponectin and leptin: adipose tissue-derived mediators of inter-organ communication. *J Lipid Res* 2019;60:1648–1684
34. Deng Z-b, Poliakov A, Hardy RW, et al. Adipose tissue exosome-like vesicles mediate activation of macrophage-induced insulin resistance. *Diabetes* 2009;58:2498–2505
35. Zhang Y, Mei H, Chang X, Chen F, Zhu Y, Han X. Adipocyte-derived microvesicles from obese mice induce M1 macrophage phenotype through secreted miR-155. *J Mol Cell Biol* 2016;8:505–517
36. Brestoff JR, Wilen CB, Moley JR, et al. Intercellular mitochondria transfer to macrophages regulates white adipose tissue homeostasis and is impaired in obesity. *Cell Metab* 2021;33:270–282.e278
37. Rosina M, Ceci V, Turchi R, et al. Ejection of damaged mitochondria and their removal by macrophages ensure efficient thermogenesis in brown adipose tissue. *Cell Metab* 2022;34:533–548.e12
38. Yoneshiro T, Wang Q, Tajima K, et al. BCAA catabolism in brown fat controls energy homeostasis through SLC25A44. *Nature* 2019;572:614–619
39. Bean C, Audano M, Varanita T, et al. The mitochondrial protein Opa1 promotes adipocyte browning that is dependent on urea cycle metabolites. *Nat Metab* 2021;3:1633–1647
40. Plubell DL, Wilmarth PA, Zhao Y, et al. Extended multiplexing of tandem mass tags (TMT) labeling reveals age and high fat diet specific proteome changes in mouse epididymal adipose tissue. *Mol Cell Proteomics* 2017;16:873–890